ACS Catalysis

Research Article

Cite This: ACS Catal. 2019, 9, 9726−9738

pubs.acs.org/acscatalysis

Cascade Conversion of Acetic Acid to Isobutene over Yttrium-Modified Siliceous Beta Zeolites

Tingting Yan,[†] Liu Yang,[†] Weili Dai,*[,†,‡] Guangjun Wu,[†] Naijia Guan,[†] Michael Hunger,[§] and Landong Li*[,†,‡]

[†]School of Materials Science and Engineering & National Institute for Advanced Materials, Nankai University, Tianjin 300350, P.R. China

[‡]Key Laboratory of Advanced Energy Materials Chemistry of the Ministry of Education, Collaborative Innovation Center of Chemical Science and Engineering, Nankai University, Tianjin 300071, P.R. China

[§]Institute of Chemical Technology, University of Stuttgart, Stuttgart 70550, Germany

Supporting Information

ABSTRACT: The one-pot conversion of acetic acid to isobutene is a promising route for isobutene production, however, the attainment of high butadiene yield in this cascade reaction is challenging. Here, Y clusters confined in siliceous Beta zeolite were constructed and applied as robust catalysts for the acetic acid to isobutene conversion with a state-of-the-art isobutene yield of 60%, which corresponds to 90% of the theoretical maximum. The reaction network and mechanism were investigated by means of several complementary methods, namely temperature-programmed surface reaction (TPSR), *in situ* ultraviolet−visible spectroscopy (UV−vis) and diffuse reflectance infrared Fourier transform spectroscopy (DRIFTS). The independent roles of weak acidic silanol groups and Lewis acidic Y species in each reaction step were elucidated. During the acetic acid conversion process, the weak acidic silanol groups and the confined Y species are both efficient in catalyzing the acetic acid ketonization and mesityl oxide hydrolysis, while the Lewis acidic Y species are highly active in catalyzing the acetone aldol condensation and mesityl oxide hydrolysis. With the synergistic effect between silanols and Y species as well as the zeolite structural confinement effects, a greatly enhanced isobutene production from acetic acid conversion could be achieved.

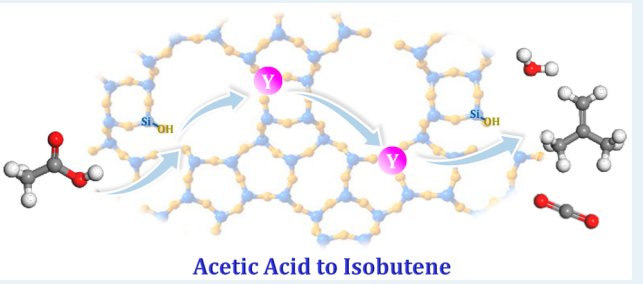

KEYWORDS: *acetic acid to isobutene, Lewis acid sites, yttrium, zeolite, reaction mechanism*

1. INTRODUCTION

Isobutene has been widely utilized as an intermediate for the production of industrial commodities, e.g., butyl rubber and ethyl *tert*-butyl ether (ETBE).[1−4] Currently, isobutene is mainly produced from the steam cracking of fossil feedstocks like napththa. With the continuous reduction of steam cracking, the traditional route to produce isobutene is difficult to meet the increasing demands of the isobutene market. In this context, it is highly desirable to explore an alternative route to produce isobutene, especially from the renewable raw materials.

During the past years, extensive attention has been attracted to the ketonization of carboxylic acids to ketones over both alkaline-earth metal oxides and transition metal oxides, and which is widely regarded as an effective method to neutralize and upgrade organic acids.[5−8] On the other hand, ketones could be further converted to alkenes via aldolization and subsequent self-deoxygenation on acidic zeolites like H-ZSM-5, H-Y, and H-Beta.[9−12] Hence, a one-pot route that couples ketonization, condensation, and cracking of bio-oil derived acetic acid into isobutene over a single catalyst is emerging. Based on the well accepted reaction route of acetone to isobutene, several key reaction steps of acetic acid to isobutene are now acknowledged (Scheme 1), including (i) the

Scheme 1. Reaction Network of the Acetic Acid to Isobutene Conversion

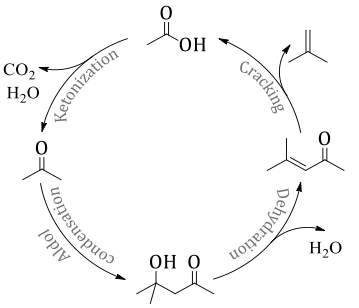

Received: July 6, 2019
Revised: September 2, 2019
Published: September 16, 2019

Downloaded via UNIV OF STUTTGART on October 17, 2019 at 12:25:41 (UTC).
See https://pubs.acs.org/sharingguidelines for options on how to legitimately share published articles.

© XXXX American Chemical Society

DOI: 10.1021/acscatal.9b02850
ACS Catal. 2019, 9, 9726−9738

ketonization of acetic acid to acetone, (ii) the aldol condensation of acetone to diacetone alcohol, (iii) the dehydration of diacetone alcohol to mesityl oxide, and (iv) the cracking reaction of mesityl oxide to isobutene and acetic acid. Obviously, this is a very complicated reaction process and catalysts with multiple functionalities are required for the one-pot conversion of acetic acid to isobutene. The key to the success of this process is the high isobutene yield for practical operation.

On the basis of above-mentioned reaction route, recently, Román-Leshkov and colleagues developed a $Zn_2Zr_8O_z$ binary metal oxide that could catalyze a multiple-step cascade reaction of acetic acid to isobutene, and an isobutene yield of 50% could be achieved.[13] The Lewis acid−base pairs of binary metal oxides are related to the acetic acid ketonization and the further aldol condensation, while the Brønsted acid sites are responsible for the hydrolysis of mesityl oxide to isobutene. However, with the presence of Brønsted acid sites, the further reactions of isobutene would also occur, leading to a rapid catalyst deactivation by losing active sites for the secondary acetone to isobutene conversion.[4,14] Very recently, Wang and colleagues also reported a sustainable way to directly produce $C_3^=$−$C_6^=$ olefins from carboxylic acids over a similar $Zn_1Zr_{10}Oz$ catalyst, but only with the Lewis acid−base functional sites.[5] Although the catalyst lifetime could be greatly prolonged with the absence of Brønsted acid sites and the olefin distribution could be well controlled by H_2 cofeeding, the isobutene yield was still on the level of ∼50%. Therefore, developing an efficient catalyst with a higher isobutene yield and understanding the structure−activity relationships at the molecular level in the one-pot acetic acid to isobutene conversion, are most desirable now, which are the aims of this work.

Our previous work demonstrated that the confined Lewis acidic Y species in siliceous Beta zeolite, i.e. [Si]Beta, exhibited the particular characteristics in the aldol condensation reaction.[15,16] Furthermore, the confinement effect of zeolite could greatly increase the chance of the intermediates to react with each other on the functional sites to generate the target product rather than escape as unwanted byproducts. Since the aldol condensation of acetone is involved in the acetic acid to isobutene conversion, the unconverted acetone intermediate could easily escape from the surface of the common oxide catalysts as the byproduct. In contrast, the confined rare earth metal clusters in [Si]Beta zeolite are expected to enhance the secondary acetone to isobutene conversion, and consequently exhibit good performance in the acetic acid to isobutene conversion.

Herein, Y/Beta catalysts were prepared via the postsynthesis route and applied in the acetic acid to isobutene conversion. The effects of the Y content, reaction temperature, and support on the catalytic performance were investigated. After optimization, a state-of-the-art isobutene yield of 60%, corresponding to 90% of the maximum theoretical yield, could be achieved over the 10% Y/Beta catalyst. The independent roles of weak acidic silanol groups and Lewis acidic Y species in each reaction step of the acetic acid to isobutene conversion and the mechanism of each step were then investigated via TPSR, TP-UV−vis, *in situ* DRIFT spectroscopy, and modulation experiments. On the basis of the catalytic and spectroscopic results, the reaction mechanism and structure−activity relationships in the acetic acid to isobutene conversion were well elucidated.

2. EXPERIMENTAL SECTION

2.1. Catalyst Preparation. Y/Beta zeolite catalysts were prepared through a two-step procedure as described elsewhere,[15] consisting of the dealumination of the parent H/[Al,Si]Beta zeolite and then introduction of Y species via wet impregnation. In a typical process, commercial H/[Al,Si]Beta zeolite with nominal n_{Si}/n_{Al} ratio of 13.5 (Sinopec Co.) was stirred in a 13 mol/L nitric acid aqueous solution at 373 K overnight to obtain a fully dealuminated [Si]Beta. The obtained powder was filtered, washed thoroughly with deionized water, and dried at 473 K overnight. Afterward, 1.0 g of the [Si]Beta host zeolite was impregnated with metal nitrates. Typically, the metal precursors (rare earth metals) were dissolved to excess water to form solution, to which [Si]Beta was added under stirring for 8 h. Then, the homogeneous slurry was evaporated at 353 K and calcined at 823 K for 6 h in flowing air. The zeolite samples after calcination were directly used as the catalysts in acetic acid to isobutene conversion without any reduction treatment. The final product was labeled by *x*%-metal/Beta, where *x* indicates the designated weight loading of metal in the sample. The Sn/Beta and Ti/Beta zeolites were prepared by a two-step metalation procedure as described elsewhere.[17,18]

For reference, Y/SiO_2 and Y/Silicalite-1 were prepared by wet impregnation of yttrium nitrate onto the SiO_2 and Silicalite-1 supports.

2.2. Catalyst Characterization. The X-ray diffraction (XRD) patterns of the as-prepared samples were recorded on a Rigaku Smartlab powder diffractometer with Cu Kα radiation (λ = 1.5418 Å) and with a scan rate of 4°/min in the region of 2θ = 5−50°.

Samples for electron microscope analysis were prepared by drying a drop of sample-containing alcohol suspension on carbon-coated copper grids. Transmission electron microscopy (TEM) images were obtained by a JEOL JEM-2800 transmission microscope with an acceleration voltage of 200 kV. Mapping the elemental distribution of zeolite catalyst was conducted under STEM mode using a JEOL built-in energy dispersive spectrum (EDS) software.

X-ray photoelectron spectra (XPS) were measured on a Thermo Scientific ESCALAB 250Xi spectrometer using monochromatic Al Kα X-ray source ($h\nu$ = 1486.6 eV) as the excitation source. High-resolution spectra were obtained by using an aperture slot of 300 × 700 μm. Accurate binding energies (±0.1 eV) were determined with respect to the position of the adventitious C 1s peak at 284.8 eV.

The solid-state MAS NMR measurements were performed on a Bruker Avance III spectrometer at resonance frequencies of 400.1 and 161.9 MHz for ^{1}H and ^{31}P nuclei, respectively. ^{1}H and ^{31}P MAS NMR spectra were obtained upon a single-pulse excitation of $\pi/2$ with a repetition time of 20 and 30 s, respectively. All ^{1}H and ^{31}P MAS NMR studies were performed with dehydrated samples, which were treated at 723 K in vacuum (below 10^{-2} Pa) for 12 h. Thereafter, the probe molecules, i.e., ammonia and TMPO, were loaded for further measurements. Loading of the dehydrated catalysts with TMPO (Alfa Aesar) was performed inside a glovebox, purged with dry nitrogen gas, by mixing ca. 50 mg of the dehydrated samples with ca. 2.5 mg TMPO inside a rotor, which was subsequently sealed with an O-ring-containing Marcor-Cap. In a further step, the TMPO-loaded samples inside the sealed rotors were heated at 533 K for 2 h for

DOI: 10.1021/acscatal.9b02850
ACS Catal. 2019, 9, 9726−9738

reaching a homogeneous distribution of the probe molecules on the sample material. The ammonia loading of the dehydrated samples was done on a vacuum line by adsorption of 100 mbar ammonia (Griesinger) at 298 K for 10 min, followed by an evacuation ($p < 10^{-2}$ mbar) at 453 K for 2 h for removing weakly physisorbed ammonia. Quantitative ^{1}H MAS NMR measurements were performed by using zeolite 35H,65Na-Y (decationization degree of 35%) as an external intensity standard. ^{1}H MAS NMR difference spectra of the unloaded and ammonia-loaded samples under study were utilized for the signal separation and the determination of the relative signal intensities. For the calculation of the number of NH_3 coordinated at Lewis acid sites, the integral intensities of the corresponding ^{1}H MAS NMR signals were divided by 3.[19]

2.3. Catalytic Evaluation. The acetic acid to isobutene conversion was investigated in a fixed-bed at atmosphere pressure. Typically, a desired amount of the catalyst (sieve fraction, 0.25−0.5 mm) was placed in a quartz reactor (5 mm i.d.) and activated under flowing nitrogen (20 mL/min) at 723 K for 1 h. After cooling to the desired temperatures, acetic acid was introduced into the system using a Kd Scientific syringe pump at a rate of 0.2 mL/h (diluted with 20 mL/min nitrogen as the carrier gas) corresponding to the weight hourly space velocity (WHSV) of 1/h. The products were analyzed by an online gas chromatograph equipped with flame ionization detector (FID) and a Poraplot Q-HT column (40 m × 0.18 mm × 0.18 μm) to separate the complicated reaction products. CO_2, CO, and CH_4 in the product were detected by Thermal Conductivity Detector (TCD) with a TDX-01 packed column, and CH_4 was used as a ligament for calibrating the percentage composition of CO_x and hydrocarbons. The acetic acid conversion and isobutene selectivity are defined as follows:

$$\text{acetic acid conversion (carbon mol\%)} = \frac{[\text{acetic acid}]_{\text{inlet}} - [\text{acetic acid}]_{\text{outlet}}}{[\text{acetic acid}]_{\text{inlet}}} \times 100\%$$

$$\text{isobutene selectivity(carbon mol\%)} = \frac{2 \times [\text{isobutene}]_{\text{outlet}}}{[\text{acetic acid}]_{\text{inlet}} - [\text{acetic acid}]_{\text{outlet}}} \times 100\%$$

2.4. Acetic Acid Temperature-Programmed Surface Reactions (TPSR). Acetic acid TPSR experiments were performed in a fixed-bed at atmosphere pressure connected with downstream gas sampling mass spectrometer (MS, Pfeiffer-Balzer Omnistar). Typically, helium was used as the carrier gas, because of its lower m/z value of 4, which has no overlap with the main products or intermediates in the acetic acid and acetone conversion.

In a typical process, 0.4 g of samples was activated at 723 K for 1 h in a helium flow (20 mL/min) and cooled to 298 K. Then, acetic acid was continuously introduced by flowing helium (20 mL/min) through a bubbler at constant temperature, and the acetic acid TPSR experiment was carried out in the temperature range of 298−773 K with a heating rate of 5 K/min. Simultaneously, acetic acid and intermediates, including acetone, diacetone alcohol, mesityl oxide, isobutene, carbon dioxide, and water, were monitored by MS in the TPSR experiment. The m/z values of the above-mentioned species were referred as 45, 58, 59, 83, 41, 44, and 18, respectively (see Table S1 for more details).[20,21]

2.5. *In Situ* Ultraviolet−Visible Spectroscopy (UV−vis) and Diffuse Reflectance Infrared Fourier Transform Spectroscopy (DRIFTS). The nature of organic intermediates formed during the acetic acid conversion was *in situ* monitored by DRIFTS and UV−vis spectroscopy as described in refs 22 and 23, respectively. The DRIFT spectra were recorded on a Bruker Tensor 27 spectrometer equipped with an *in situ* reaction chamber and a liquid N_2 cooled high sensitivity MCT detector. Prior to the DRIFT experiments, ca. 20 mg of catalyst was finely ground and placed in the chamber. Then, the catalyst was pretreated at 723 K for 1 h in flowing argon gas (20 mL/min). Subsequently, the temperature was decreased to the desired value to take a blank spectrum as the background. After importing the background, acetic acid was fed onto the catalyst surface with a WHSV of 1/h, and the time-resolved spectra were recorded with a resolution of 4 cm^{-1} and an accumulation of 128 scans.

UV−vis spectra were recorded via a PerkinElmer Lambda 750 UV−vis−NIR spectrometer equipped with an *in situ* reaction chamber. The UV−vis spectra were recorded in the diffuse reflection mode with the range of 200−600 nm. Prior to UV−vis experiments, ca. 20 mg of catalyst was placed in the chamber and activated at 723 K for 1 h in flowing argon gas (20 mL/min). Then, reference UV−vis spectra of the fresh catalyst were recorded at reaction temperature prior to starting the acetic acid flow.

3. RESULTS AND DISCUSSION

3.1. Catalytic Performance of the As-Prepared Catalysts. The acetic acid to isobutene conversion over various rare-earth metal-modified zeolite catalysts was first investigated in a fixed-bed reactor at 723 K for TOS = 30 min. First, blank experiment was carried out at different temperatures using quartz instead of catalysts, confirming that no homogeneous noncatalytic reaction occurs. A 95% carbon balance was observed for acetic acid conversion over all the as-prepared catalysts unless otherwise noted. As shown in Figure 1, all the rare-earth metals, i.e., Sc, Y, La, Ce, and Pr, appear to

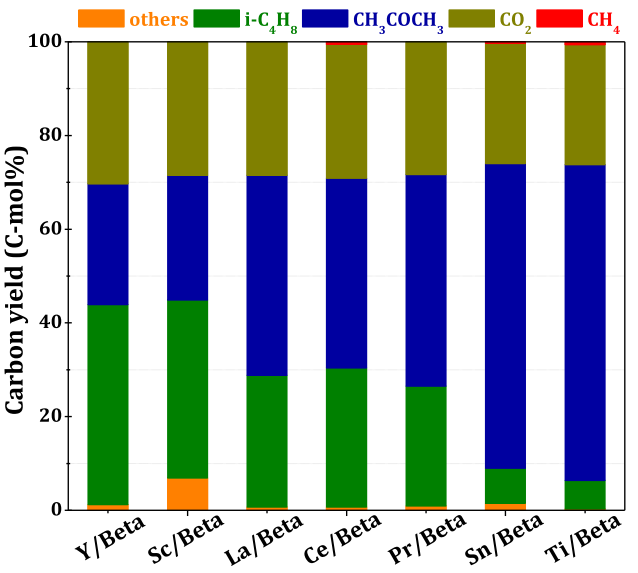

Figure 1. Product yields in the acetic acid to isobutene conversion over different catalysts. Reaction conditions: reaction temperature = 723 K, WHSV = 1/h, 5 wt% metal loadings, TOS = 30 min.

DOI: 10.1021/acscatal.9b02850
ACS Catal. 2019, 9, 9726−9738

be active for the acetic acid to isobutene conversion, and a high isobutene selectivity of 42.7% could be achieved over the Y/Beta zeolite catalyst. In comparison, Sn- and Ti-containing Beta zeolites that are generally utilized as the solid Lewis acids in many reactions including the alkene epoxidation and the ring-opening hydration of epoxides,[17,18] however, only exhibit a negligible activity in the acetic acid to isobutene conversion under study. In order to get more insight into the acetic acid to isobutene reaction, more detailed studies were performed on Y/Beta catalysts.

The effects of the Y contents and reaction temperatures on the acetic acid conversion and product distribution were further investigated, and the results are given in Figure 2. It is

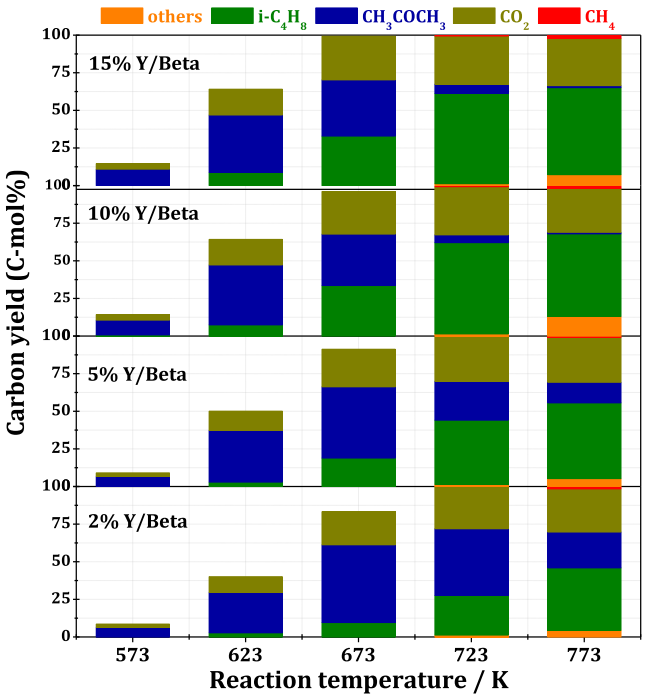

Figure 2. Product yields in the acetic acid to isobutene conversion over different Y/Beta catalysts. Reaction conditions: reaction temperature = 573−773 K, WHSV = 1.0/h, TOS = 30 min.

clear that the Y contents of the catalyst show a strong impact on the catalytic performance. At the low reaction temperatures of 573−623 K, a gradual increase of acetone yield was observed with increasing Y loading from 2 to 15%, indicating that Y species are beneficial to the acetone production to a certain extent. This is in line with the catalytic performance of acetic acid conversion over bulk Y_2O_3 (Figure 3a), where Y species are the active sites for the acetone production. At higher reaction temperatures of 673−773 K, an obvious increase of the isobutene yield could be obtained with the increase of the Y loading from 2 to 10%, hinting that Y species are the dominant active sites for the isobutene production. However, with the further increase of the Y loading from 10 to 15%, no obvious influence on the isobutene yield was observed. This indicates that approaching saturation of highly dispersed Y species associated with the evolution of the silanols already occurs on 10% Y/Beta zeolite. For a particular sample, e.g., 10% Y/Beta, acetic acid conversion gradually increases with increasing reaction temperature, and reaches about 100% at 723 K. Simultaneously, the isobutene yield also gradually increases at the expense of the acetone yield, hinting that acetone is an intermediate in the acetic acid to isobutene conversion. When the reaction temperature increased to 773 K, trace amount of CH_4 originated from acetic acid decarboxylation[24] and small amounts of alkenes (C2, C3, and *n*-C4), due to the isomerization, metathesis, and cracking of isobutene,[25−27] appeared in the products. Therefore, 10% Y/Beta and a reaction temperature of 723 K were optimized for the reaction, and a state-of-art isobutene yield of 60%, which corresponds to 90% of the theoretical yield (66.7% on a carbon basis), could be achieved under employed conditions.

According to our previous studies, the interaction between the metal species and support can greatly influence the catalytic performance.[15] In order to compare the effect of support on the catalytic performance of Y-modified catalysts in the acetic acid conversion, the temperature dependence of the product yield over the bare supports and bulk Y_2O_3 were investigated. As shown in Figure 3a, acetone and CO_2 originated from the ketonization of acetic acid, are the dominate products over all the samples in the temperature range of 573−773 K, indicating that the ketonization of acetic acid could proceed over all the bare supports and the bulk Y_2O_3, in line with previous studies.[7,8,21,28−30] After the introduction of Y species, i.e., on Y-modified catalysts, similar variation trends of the acetone yields to those obtained on the bare supports were observed in the low reaction temperature range of 573−623 K (Figure 3b), but the isobutene yields differed a lot. For Y/Beta, a significant amount of isobutene appeared in the products. While for Y/Silicalite-1 and Y/SiO_2, only the yields of acetone and CO_2 were enhanced, besides this, no any isobutene appeared at the low reaction temperature. However, when increasing the reaction temperature to over 723 K, a large amount of isobutene also appeared over Y/SiO_2, but was still not observed over Y/Silicate-1. It clearly indicates that the supports have a strong impact on the catalytic performance of Y-modified catalysts during the acetic acid to isobutene conversion, and their different catalytic performance may be due to the interaction between the Y species and supports, which is also indicated by the Y 3d XPS results. In the Y 3d XPS spectra (Figure 3c), signals of binding energy values at 160.5 and 158.4 eV corresponding to Y 3d5/2 and 3d3/2, respectively, occurred for Y/Beta, which are distinctly higher than that for bulk Y_2O_3 (158.3 and 156.4 eV) due to the formation of Si−O−Y bonds.[15] While for Y/SiO_2 and Y/Silicate-1, the Y 3d binding energy values gradually shifted toward higher values compared to bulk Y_2O_3, but were still distinctly lower than Y/Beta. This could be explained from the weaker interaction between Y and SiO_2 as well as Silicalite-1 or the formation of Si−O−Y bonds on these supports. Therefore, the highest isobutene yield of 60% can be achieved on Y/Beta with the strong interaction between Y species and [Si]Beta, followed by Y/SiO_2 and Y/Silicalite-1 with isobutene yields of 19.6% and 0.8%, respectively, due to the weak interaction between Y species and the corresponding supports.

3.2. Optimization of the Reaction Temperature and the Stability of the Optimum Catalyst. As shown in Figure 2, the product distribution is sensitive to the reaction temperature during the acetic acid to isobutene conversion. Therefore, the reaction temperature of the acetic acid to isobutene conversion was further optimized in the range of 673−773 K. As shown in Figure 4a, nearly 100% acetic acid conversion is obtained in the temperature range of 673−773 K. At 673 K, the unconverted acetone is observed as the dominating product. With increasing reaction temperature, the

DOI: 10.1021/acscatal.9b02850
ACS Catal. 2019, 9, 9726−9738

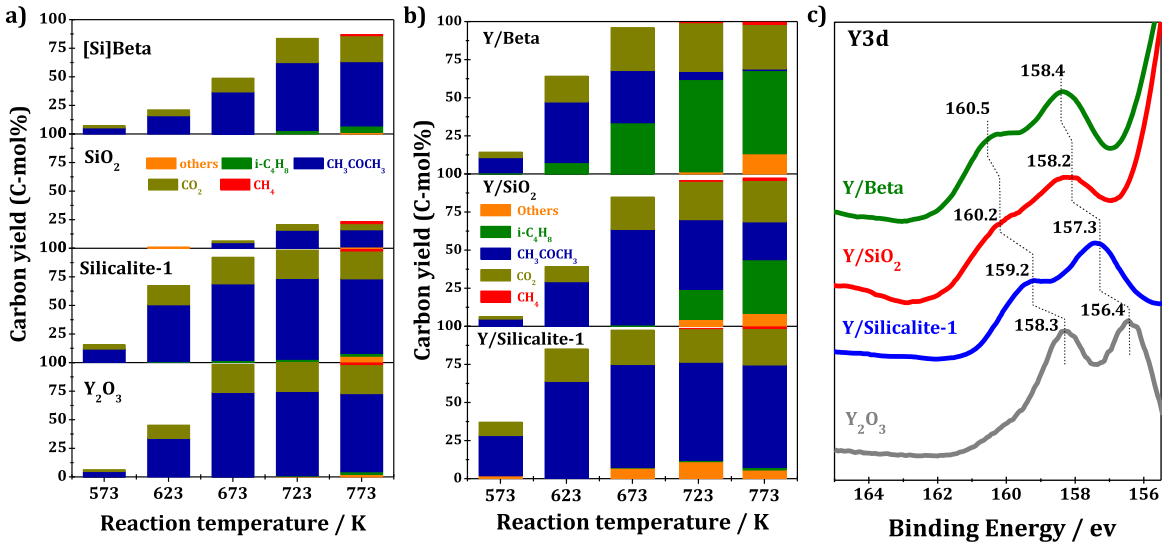

Figure 3. Product yields in the acetic acid conversion over the bare supports, bulk Y_2O_3 (a) and Y-modified catalysts (b). Reaction conditions: reaction temperature = 573−773 K, WHSV = 1.0/h, TOS = 30 min. (c) Y 3d XPS of Y-modified catalysts, and reference Y_2O_3 samples.

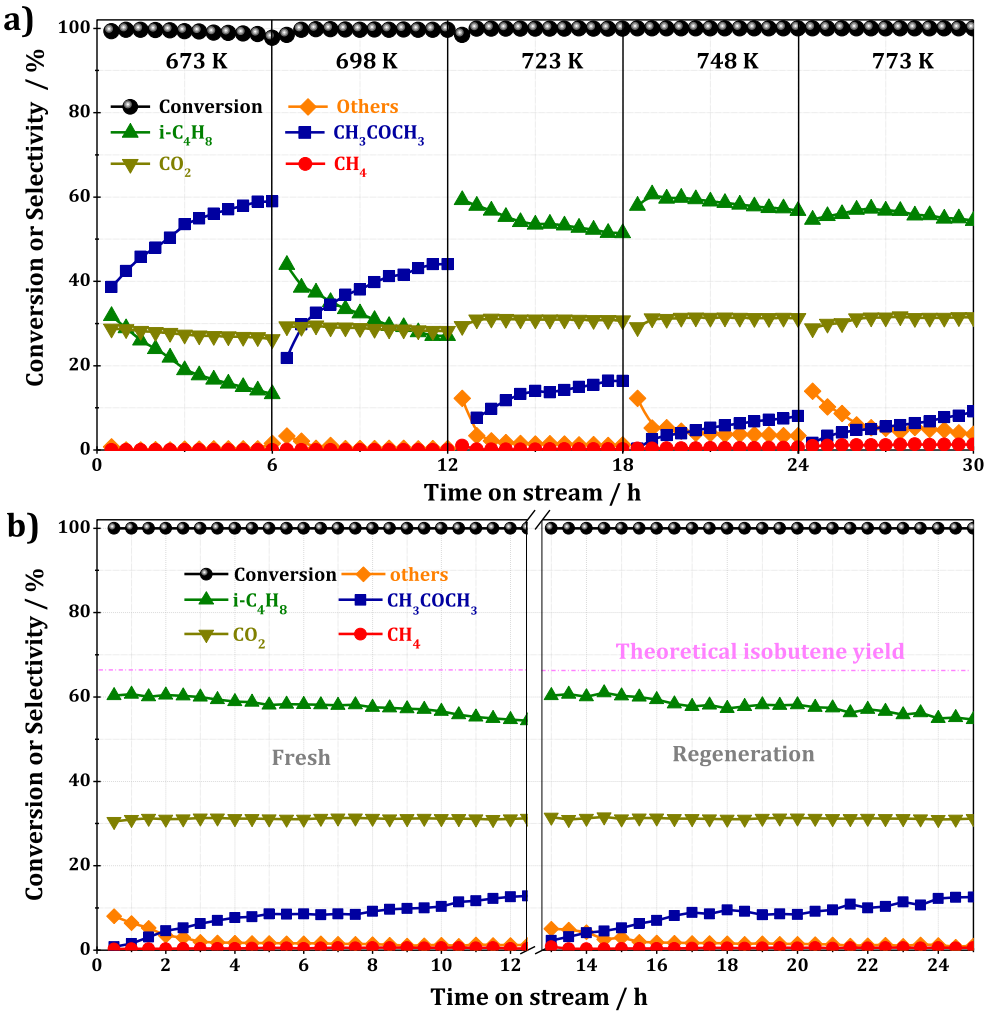

Figure 4. (a) Acetic acid conversion and product selectivity over the 10% Y/Beta catalyst. Reaction conditions: reaction temperature = 673−773 K, WHSV = 1.0/h, TOS = 6.0 h. (b) Catalytic properties of generated 10% Y/Beta zeolite used as acetic acid to isobutene catalyst at 748 K with a TOS of 12.5 h.

initial selectivity to isobutene gradually enhances, and simultaneously, an obvious decline in the selectivity to acetone occurs. It indicates that the further conversion of acetone to isobutene needs to overcome a high activation energy barrier.

DOI: 10.1021/acscatal.9b02850
ACS Catal. 2019, 9, 9726−9738

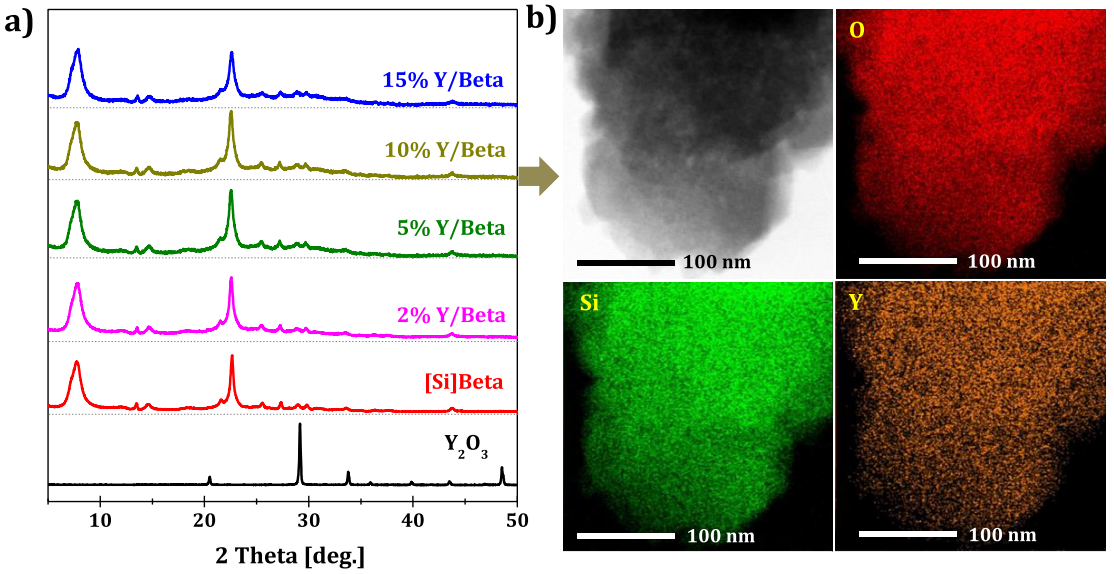

Figure 5. (a) XRD patterns of Y_2O_3, [Si]Beta, and different Y/Beta catalysts. (b) STEM images of Y/Beta with corresponding element mapping.

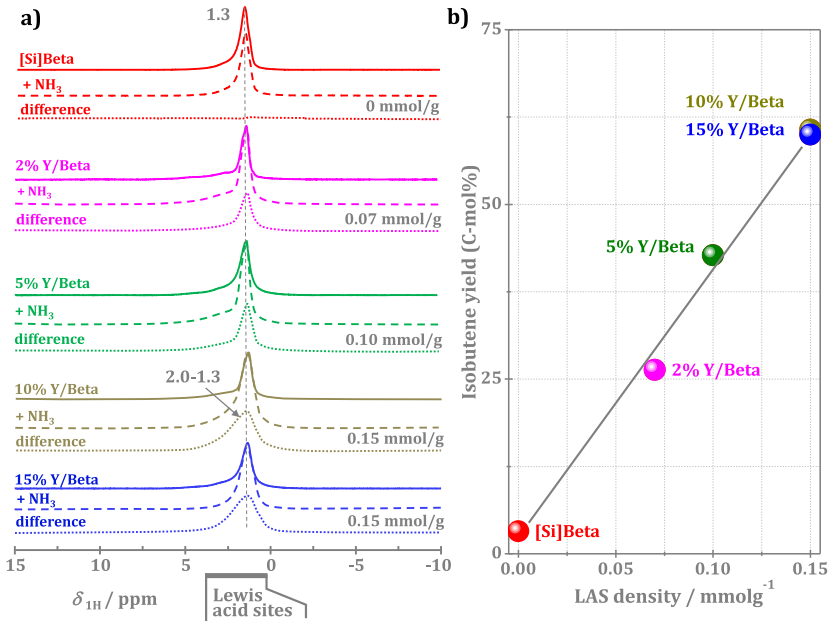

Figure 6. (a) ^{1}H MAS NMR spectra of dehydrated [Si]Beta and Y/Beta zeolites recorded before (top) and after (medium) adsorption of ammonia. The bottom spectra (difference) were obtained via subtracting the top spectra (dehydrated) from the medium spectra (after NH_3 adsorption). (b) Isobutene yield plotted as the density of Lewis acid sites (LAS) of the samples.

When increasing the reaction temperature to 748 K, a high isobutene yield of ~60% with a good stability could be achieved. The further increase of the reaction temperature would lead the formation of CH_4 and other alkenes, and consequently, cause a little decline of the isobutene yield. On the other hand, a stable selectivity to CO_2 of ~30% occurred in the whole temperature range of 673−773 K, indicating a full ketonization reaction of acetic acid to acetone at these temperatures.

Under optimum reaction conditions (*vide supra*), i.e., 10% Y/Beta and a reaction temperature of 748 K, the durability and regeneration of the catalyst were investigated. As shown in Figure 4b (left), 100% acetic acid conversion with a slight decrease in isobutene selectivity can be observed over the fresh sample during the acetic acid to isobutene conversion. Simultaneously, the selectivity to acetone gradually increases, indicating that the Y species responsible for the isobutene formation are gradually covered by coke compounds, which can be supported by the regeneration results. As shown in Figure 4b (right), the acetic acid conversion and product selectivities could be well recovered after the regeneration.

3.3. Physico-chemical Properties of the Y/Beta Zeolite Catalysts. For a better understanding the textual properties of the Y/Beta catalysts, the XRD patterns of the parent [Si]Beta and the Y/Beta samples are collected in Figure 5a. Typical diffraction lines characteristic of the BEA topology could be observed for all the samples, indicating that the primary BEA structure was well preserved after the Y modification.[31] Additionally, no obvious diffraction lines due to Y species (Y_2O_3, JCPDS: 76-0151) occur on the Y/Beta

DOI: 10.1021/acscatal.9b02850
ACS Catal. 2019, 9, 9726−9738

zeolites, indicating that the Y species, amorphous or very small, are highly dispersed within the [Si]Beta matrix. This finding was supported by STEM images and the corresponding element mapping results, as the homogeneous distribution of Y species and no obvious Y-containing aggregates appear on the 10% Y/Beta zeolite (Figure 5b).

On the basis of our previous work, the dealumination of H/[Al,Si]Beta and incorporation of Ti, Sn, Zr, and Ce species were associated with the evolution of silanols related to the vacant sites during the postsynthesis.[17,18,32,33] This phenomenon also occurred on Y/Beta zeolites prepared via the wet impregnation method under study. The DRIFT spectrum (Figure S1) of parent H/[Al,Si]Beta exhibits two obvious characteristic bands in hydroxyl stretching region: one band at 3740 cm^{-1} due to isolated external Si−OH groups, and the other band at 3600 cm^{-1} assigned to bridging hydroxyls Si−OH−Al.[31] After the dealumination, the band (3600 cm^{-1}) ascribed to bridging hydroxyls Si−OH−Al disappeared, and simultaneously, the intensification of the band at 3735 cm^{-1} due to isolated internal Si−OH groups and a broad band at 3520 cm^{-1} attributed to hydrogen-bonded silanol groups occurred. This finding indicates the complete elimination of Al from the Beta zeolite framework and the formation of vacant T atom sites, in accordance with our earlier results.[17] After the introduction of Y species, an obvious decrease in the intensities of Si−OH bands at 3735 and 3520 cm^{-1} occurred, evidencing that confined Y species were associated with the evolution of the silanols, in accordance with the Y 3d XPS results (Figure 3c).

The hydroxyl groups in [Si]Beta zeolites before and after the introduction Y species were further analyzed by ^{1}H MAS NMR spectroscopy. As shown in Figure 6, a dominant signal at δ_{1H} = 1.3 ppm due to silanol groups at framework defects occurs on [Si]Beta zeolite. After ammonia loading, nearly no changes of the ^{1}H MAS NMR spectra could be observed, which shows that neither Brønsted nor Lewis acid sites are present in [Si]Beta zeolite. This finding indicates a complete elimination of Al from the Beta zeolite framework. After the introduction of Y species, no obvious changes of the ^{1}H MAS NMR spectra occurred for all the Y/Beta samples. However, an obvious increase of the ^{1}H MAS NMR signal intensities in the range of 1.3−2.0 ppm could be observed after the ammonia loading. According to our previous report,[16] these signals are due to ammonia molecules coordinated at Lewis acid sites. On the other hand, no ^{1}H MAS NMR signals of ammonium ions at 6−7 ppm due to the protonation of the ammonia molecules at Brønsted acid sites appeared. These observations evidence that the introduction of Y species into the [Si]Beta zeolite only leads to the formation of Lewis acid sites. The quantitative evaluation of the signals at 1.3−2.0 ppm provided the densities of accessible Lewis acid sites in the Y/Beta samples. The densities of accessible Lewis acid sites were calculated to be 0, 0.08, 0.10, 0.15, and 0.15 mmol/g for the [Si]Beta, 2% Y/Beta, 5% Y/Beta, 10% Y/Beta, and 15% Y/Beta, respectively. These data correlate well with the isobutene yields (Figure 6b), evidencing that the Lewis acid sites generated from incorporated Y species are responsible for the isobutene formation during the acetic acid to isobutene conversion.

To support the assignment of the nature of surface sites on the Y/Beta samples under study, trimethylphosphine oxide (TMPO) was also utilized as a probe molecule. The ^{31}P MAS NMR spectra of the dehydrated samples after TMPO loading are shown in Figure 7. For [Si]Beta, a dominating signal at 41 ppm occurs, which is due to the physisorbed TMPO at weak acidic silanol groups. In contrast, for the Y/Beta samples, besides the weak signals at about 41 ppm, new signals owing to TMPO adsorbed at the Lewis acid sites occur at ∼52 ppm,[19] which agrees well with the ^{1}H MAS NMR results.

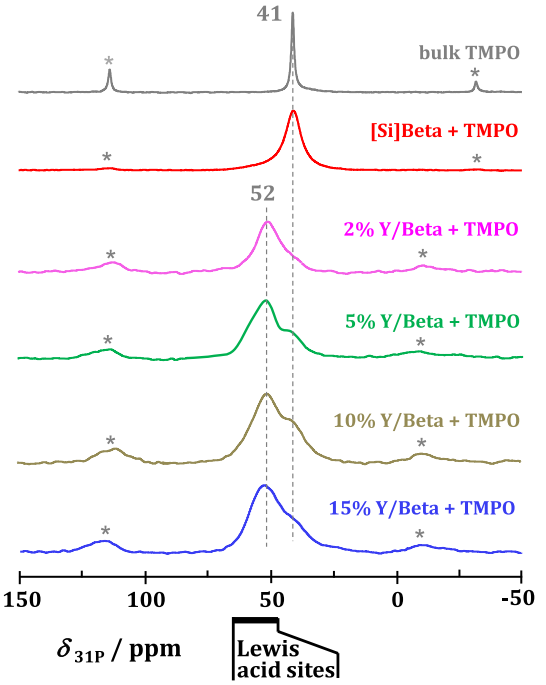

Figure 7. ^{31}P MAS NMR spectra of bulk TMPO and TMPO-loaded [Si]Beta and Y/Beta zeolites. Asterisks denote spinning sidebands.

Summarizing the characterization of surface sites by DRIFT and solid-state NMR spectroscopy, we come to the conclusion that the Y species in the Y/Beta catalysts under study are associated with the evolution of the silanol groups in these zeolites, which lead to the formation of Lewis acid sites. Furthermore, these Lewis acid sites are responsible for the isobutene formation, and the densities of which correlate well with the isobutene yields during the acetic acid to isobutene conversion.

3.4. Temperature-Programmed Surface Reaction (TPSR) Experiments and Ultraviolet−Visible (TP-UV−Vis) Spectroscopy. To gain deeper insight into the reaction route of the acetic acid to isobutene conversion over Y/Beta zeolite, several complementary experimental approaches were performed. First, acetic acid TPSR was utilized to investigate the possible products or intermediates during the reaction. The compounds monitored by MS, i.e., acetone (m/z = 58), diacetone alcohol (m/z = 59), mesityl oxide (m/z = 83), and isobutene (m/z = 41), were selected according to the reaction route as shown in Scheme 1. In addition to the m/z signals of the above-mentioned major species, the m/z signals of acetic acid (m/z = 45), carbon dioxide (m/z = 44), and water (m/z = 18) were also monitored for comparison.

In Figure 8a, the TPSR profiles obtained for Y/Beta under a constant acetic acid flow are shown. The acetic acid curve starts to decrease at about 480 K, and simultaneously the acetone and carbon dioxide curves slop upward. This finding indicates the occurrence of acetic acid ketonization ($2CH_3COOH \rightarrow CH_3COCH_3 + CO_2 + H_2O$), which is the initial reaction step during the acetic acid to isobutene conversion at low reaction temperatures.[7,24,28] With the

DOI: 10.1021/acscatal.9b02850
ACS Catal. 2019, 9, 9726−9738

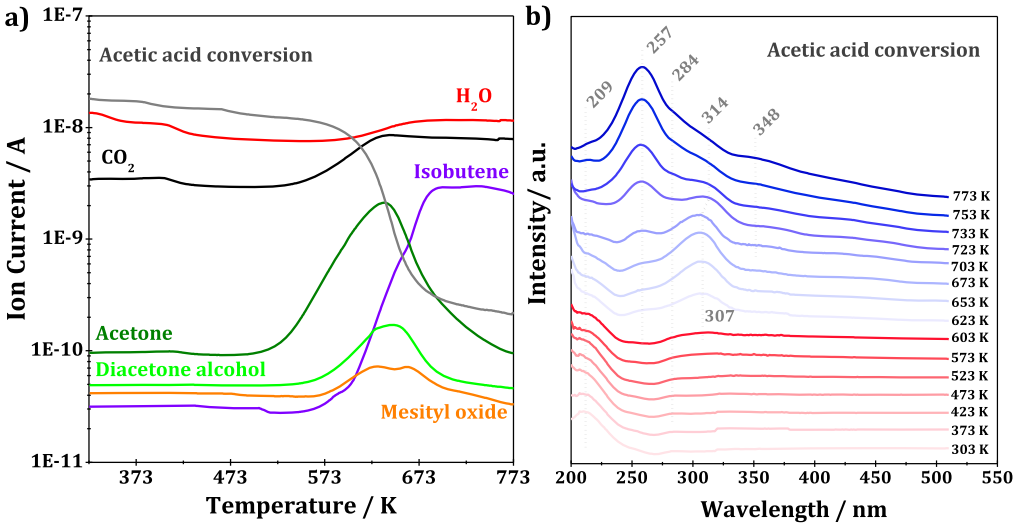

Figure 8. (a) Temperature-programmed surface reaction (TPSR) profiles and UV−vis spectra (b) recorded during the acetic acid to isobutene conversion under a constant acetic acid stream over 10% Y/Beta zeolite. Reaction conditions: WHSV = 1/h, temperature of T = 303−773 K.

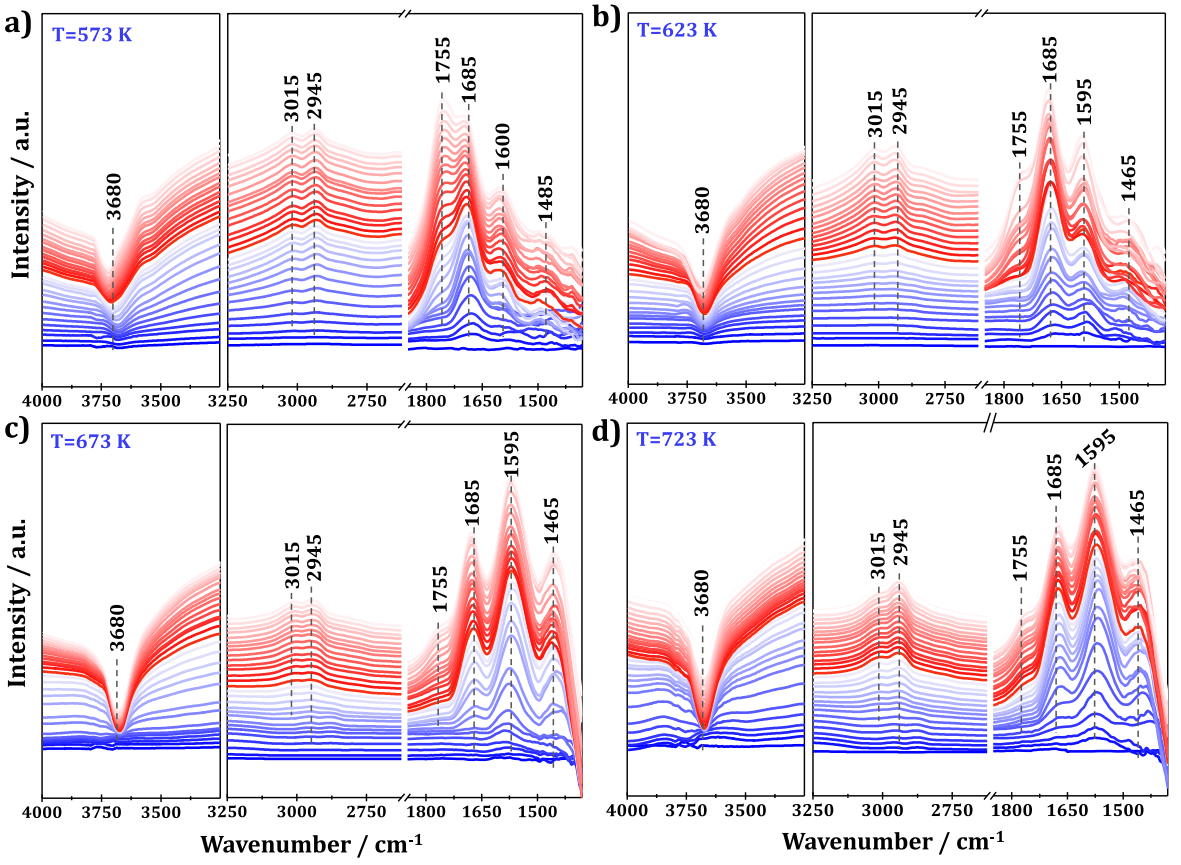

Figure 9. *In situ* FTIR spectra recorded during the acetic acid conversion over Y/Beta catalyst at different reaction temperatures: (a) 573 K, (b) 623 K, (c) 673 K, and (d) 723 K. Reaction conditions: WHSV = 1.0/h.

increasing reaction temperature to about 553 K, diacetone alcohol and mesityl oxide start to appear and exhibit the same variation trend, hinting to the occurrence of the acetone aldol condensation reaction and a further dehydration reaction of diacetone alcohol to mesityl oxide. Meanwhile, a slight increase of water can also be observed, well supporting the occurrence of the dehydration reaction. Subsequently, isobutene starts to appear, and gradually reaches an equilibrium, when the temperature further increases to over 673 K. Simultaneously, the curves of acetic acid, acetone, diacetone alcohol, and mesityl oxide rapidly decrease, illustrating the occurrence of the acetic acid to isobutene conversion at high reaction temperature, in line with the steady-state reaction results (Figure 2.

To get more information about the surface species formed over Y/Beta catalyst, TP-UV−vis spectroscopy was further performed. After saturation with acetic acid at 303 K, the Y/Beta catalyst was purged by argon to remove the gas phase and

DOI: 10.1021/acscatal.9b02850
ACS Catal. 2019, 9, 9726−9738

physically adsorbed acetic acid molecules. Subsequently, the chamber temperature was gradually raised from 303 to 773 K with the heating rate of 5 K/min. The UV−vis spectra obtained after subtraction of the background (fresh catalyst) are given in Figure 8b.

At T = 303 K, a dominating UV−vis band at 209 nm, due to the weakly adsorbed acetic acid (n→π^*), occurred during the acetic acid conversion (Figure 8a). When the temperature increased to 523 K, a new weak band at about 284 nm assigned to acetone appeared (Figure S2). This assignment could be supported by the adsorption of pure acetone at room temperature, which led to the appearance of one band at 284 nm (Figure S2). This indicates the occurrence of acetic acid ketonization, in good agreement with the TPSR results (Figure 8. With the further increase of temperature to over 623 K, two new bands attributed to diacetone alcohol occurred at 257 and 307 nm. This assignment is well supported by the adsorption of pure diacetone alcohol at room temperature, which led to the occurrence of two bands at 257 and 307 nm (Figure S2). These observations confirm the aldol condensation of acetone to diacetone alcohol. When the reaction temperature increased to over 723 K, the intensities of the band at 257 nm dramatically increased, and simultaneously, the band at 307 nm has shown a red shift to ∼314 nm. This could be due to the gradual conversion of diacetone alcohol to mesityl oxide, as the adsorption of pure mesityl oxide on Y/Beta gives two bands at 257 and 314 nm (Figure S2). These findings are in good agreement with the mechanistic hypothesis shown in Scheme 1. In addition, a weak broad band at ∼348 nm occurred when the reaction temperature increased to more than 703 K. According to our previous reports, this band could be assigned to large unsaturated aldehydes/ketones originated from an excessive condensation of acetone.[22]

To summarize the acetic acid TPSR and TP-UV−vis results, we conclude that the acetic acid ketonization is the first step of the acetic acid to isobutene conversion, and the formed acetone is rapidly involved in a subsequent aldol condensation reaction and leads to the formation of diacetone alcohol. Subsequently, mesityl oxide and isobutene are formed successively, which is in line with the mechanistic hypothesis shown in Scheme 1.

3.5. *In Situ* Diffuse Reflectance Infrared Fourier Transform Spectroscopy (*In Situ*-DRIFTS). To further compare surface intermediates and gas-phase products formed during the acetic acid to isobutene conversion at a desired temperature, *in situ* DRIFTS experiments were performed (Figure 9. In the spectra recorded during the acetic acid to isobutene conversion on Y/Beta catalysts in the temperature range of 573−723 K, there is one broad negative band at high wavenumber of 3680 cm^{-1}, hinting to an interaction between acetic acid and silanol groups.[16] In addition, similar bands at about 2945 and 3015 cm^{-1}, due to ν(C−H) vibrations of the acetic acid molecules, also occur in the spectra recorded at different temperatures.[34]

However, there are significant differences in the IR bands recorded at different temperatures in the spectral range of 1800−1400 cm^{-1}. At 573 K, a weak band at 1685 cm^{-1} occurred during the initial process of the acetic acid conversion. According to previous studies, this band can be attributed to the ν(C = O) of acetone, diacetone alcohol or mesityl oxide adsorbed on Lewis acid sites.[35,36] However, the appearance of mesityl oxide cannot be definitely confirmed solely based on this band, as its typical ν(C−H) and ν(C═C) vibrations (bands at 3015 and 1595 cm^{-1}) are absent. Therefore, the appearance of this band only indicates the formation of acetone, namely the occurrence of acetic acid ketonization, in good agreement with the TPSR results (Figure 8a). With the progress of acetic acid conversion, new bands at 1755, 1600, and 1485 cm^{-1} appeared. The former band at 1755 cm^{-1} is due to the ν(C═O) of the unconverted acetic acid molecules bound to catalyst surface.[34] The band at 1600 cm^{-1} together with the bands at 1685 and 3015 cm^{-1} could be explained by the formation of mesityl oxide, hinting to the occurrence of acetone aldol condensation. This assignment could be supported by the adsorption of pure acetic acid, acetone, diacetone alcohol, and mesityl oxide at room temperature, which led to the appearance of the bands at 1755, 1685, and 1595 cm^{-1}, respectively (Figure S3). On the other hand, the band at 1485 cm^{-1} can be attributed to the heavier carbon species, e.g., phorone and isophorone,[37] probably responsible for the gradual blockage of the active sites and, consequently, for the catalyst deactivation.[11,38−40] This result indicates the occurrence of further acetone aldolization and secondary mesityl oxide reactions at elevated temperatures. In the previous study, the band at 1485 cm^{-1} could be also assigned to the ν(COO−) vibration of carbonate/acetate, which are formed from the surface oligomers (e.g., phorone and isophorone).[35,41,42] With the increase of the reaction temperature to 623 K, the ratio of the band intensities at 1755 cm^{-1} (ν(C═O) of acetic acid) to 1685 cm^{-1} (ν(C═O) of acetone, diacetone alcohol or mesityl oxide) declined sharply, due to the higher acetic acid conversion, which in line with the catalytic results (Figure 2. Simultaneously, the intensities of the bands of mesityl oxide and other oligomers (1595 and 1465 cm^{-1}) greatly increased, indicating that the acetone formed during the initial period of acetic acid conversion is rapidly involved in the subsequent aldol condensation reaction at the reaction temperature of 623 K. Upon further increasing the reaction temperature to over 673 K, mesityl oxide and other oligomers (1595 and 1465 cm^{-1}) become the dominating surface species, which can also be supported by the intensified ν(C−H) vibrations at 2945 cm^{-1} (Figure 9d) and which is also in good agreement with the UV−vis results (Figure 8b). However, only trace amount of mesityl oxide occurred in the gas phase products at this temperature (Figure 8a), suggesting that mesityl oxide or the heavier oligomers formed during the acetic acid conversion, strongly adsorbed on the Y/Beta surface even at the high reaction temperature. These organic species could gradually cover the active sites and consequently cause the catalyst deactivation.[11,22,38−40] On the other hand, this can well explain the recovered catalytic activity of the regenerated catalyst (Figure 4b), as the deactivating species can be removed from catalyst surface via simple calcination.

3.6. Roles of the Active Sites in the Acetic Acid to Isobutene Conversion. The above-mentioned spectroscopic results confirm the formation of acetone, diacetone alcohol, and mesityl oxide during the acetic acid to isobutene conversion. It has been proposed that Lewis acid−base pairs contribute to the acetic acid ketonization and the further aldol condensation, and Brønsted acid sites are related to the hydrolysis activity of mesityl oxide to isobutene.[1,9,10,43] According to the catalytic results shown in Figure 3a, we can confirm that silanol groups and even bulk Y_2O_3 species are effective for acetic acid ketonization ($2CH_3COOH$ →

DOI: 10.1021/acscatal.9b02850
ACS Catal. 2019, 9, 9726−9738

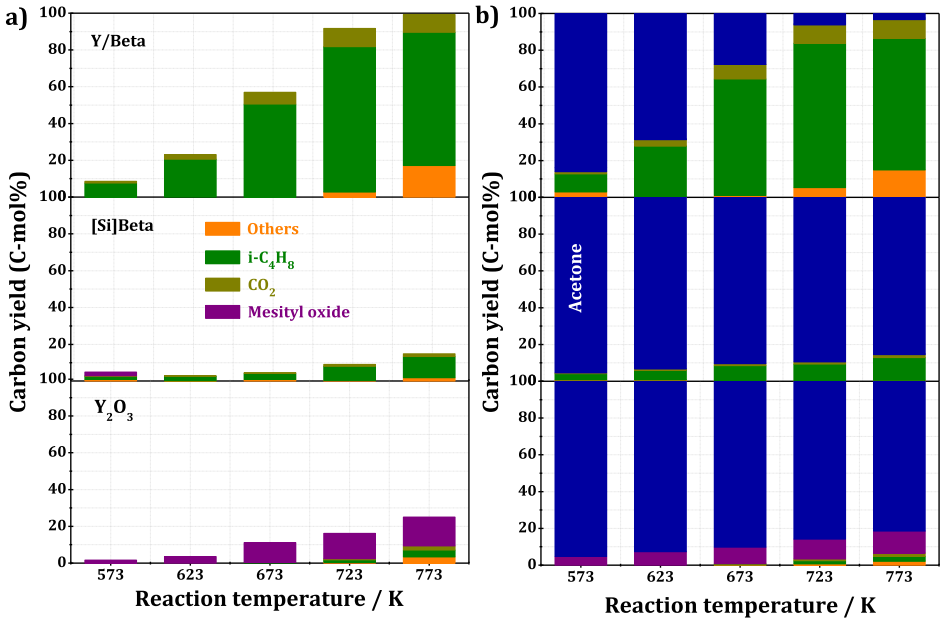

Figure 10. Product yields during the acetone (a) and diacetone alcohol (b) conversion over Y/Beta, [Si]Beta, and Y_2O_3 catalyst. Reaction conditions: reaction temperature = 573−773 K, WHSV = 1.0/h.

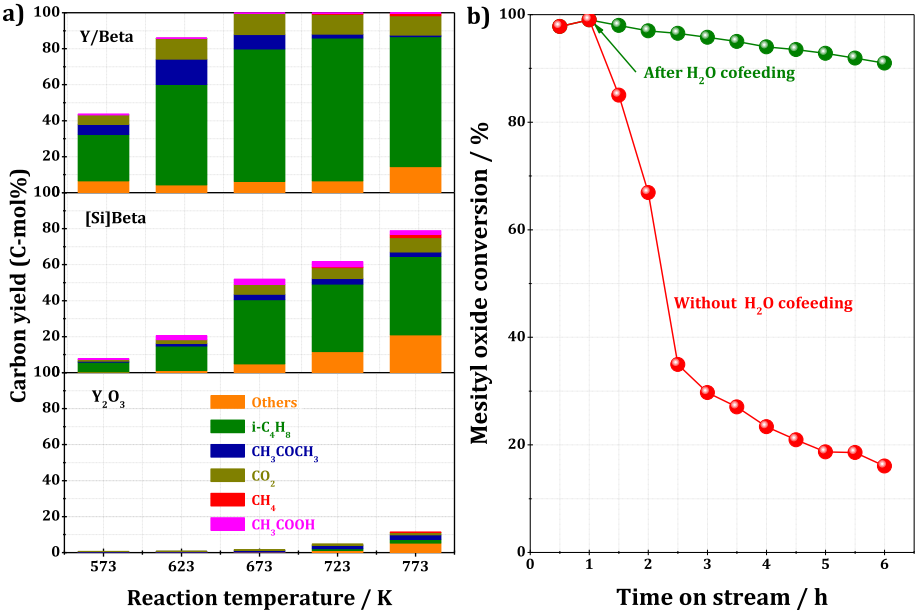

Figure 11. (a) Product yields during the mesityl oxide conversion over Y/Beta, [Si]Beta, and Y_2O_3 catalyst. Reaction conditions: reaction temperature = 573−773 K, WHSV = 1.0/h, TOS = 1.0 h. (b) The mesityl oxide conversion over Y/Beta catalyst. Reaction conditions: reaction temperature = 723 K, WHSV = 1.0/h.

$CH_3COCH_3 + CO_2 + H_2O$), i.e., the initial reaction step of the acetic acid to isobutene conversion. For the further conversion of acetone to isobutene, however, the active sites responsible for each step are still not clear. To clarify the functional sites of Y/Beta zeolites in the acetone to isobutene conversion in the absence of Brønsted acid sites, further studies of the conversion of acetone, diacetone alcohol, and mesityl oxide at different temperatures were performed in parallel on [Si]Beta, Y/Beta, and Y_2O_3.

As shown in Figure 10a, Y/Beta containing Lewis acidic Y species exhibits a remarkable activity in the acetone to isobutene conversion. In contrast, over [Si]Beta with exclusive silanol groups, the acetone conversion is extremely low. Nevertheless, the occurrence of trace amount of mesityl oxide (573 K) and isobutene (623−773 K) in the products indicates that the acetone aldol condensation and further cracking reactions could also happen with the silanol groups at high reaction temperatures. For bulk Y_2O_3, mesityl oxide was observed as the dominant product formed in the temperature range of 573−773 K. This finding indicates that the aldol condensation of acetone can take place over Y_2O_3, but the further cracking of mesityl oxide is hard to realize. These observations are well supported by the diacetone alcohol conversion over Y/Beta, [Si]Beta, and Y_2O_3 catalysts (Figure 10b), as the product distributions, e.g. isobutene and mesityl oxide, are nearly the same as those found for the acetone

DOI: 10.1021/acscatal.9b02850
ACS Catal. 2019, 9, 9726−9738

Scheme 2. Proposed Reaction Mechanism of Acetic Acid to Isobutene over Y/Beta Catalyst

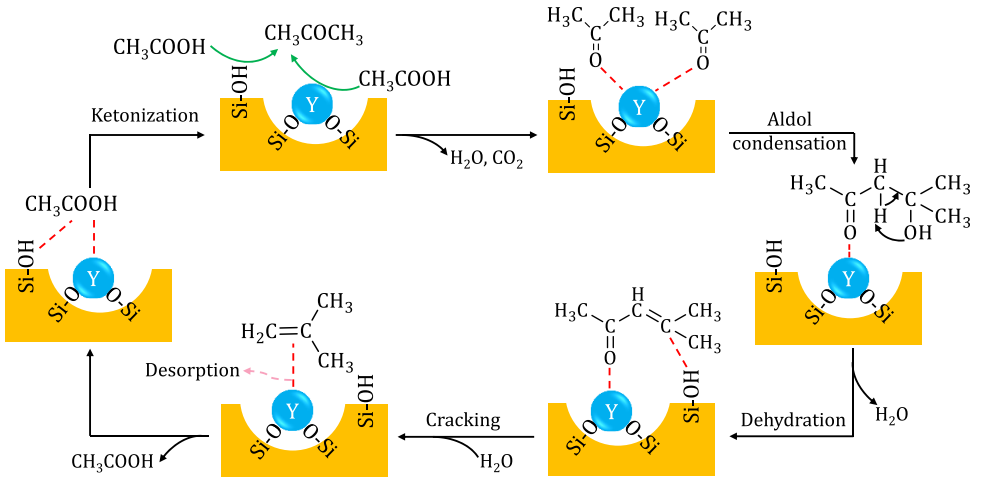

conversion. This observation illustrates that diacetone alcohol is an intermediate species during the formation of mesityl oxide, in line with the proposed reaction route in Scheme 1. In addition, the appearance of a large amount of acetone during the diacetone alcohol conversion indicates that this reaction reaches equilibrium conditions.[10,40]

According to the previous reports of McAllister,[44] Crisci,[13] Baylon[5] and their co-workers, Brønsted acid sites are essential in the cleavage of mesityl oxide, i.e., the last step of acetic acid to isobutene conversion. In the present study, the weak acidic silanol groups of [Si]Beta were proved to be active in the mesityl oxide to isobutene conversion (Figure 11a). Bulk Y_2O_3, however, was inactive in this process. After the introduction of Y species into [Si]Beta, i.e., on Y/Beta zeolite, an obvious enhancement in the isobutene yield could be achieved. These observations clearly illustrate that the silanol groups and the confined Y species in Y/Beta zeolite are both active in the cleavage of mesityl oxide to isobutene, and their combination could greatly enhance the isobutene yield. In addition, the participation of water is essential in this process, i.e., the cleavage of mesityl oxide, actually, is a hydrolysis reaction, in line with the proposed reaction route in Scheme 1. This statement can also be supported by water cofeeding experiments, where the stability of Y/Beta catalyst in the mesityl oxide to isobutene conversion could be greatly promoted.

3.7. Mechanistic Interpretation over Y/Beta Catalyst.

As a demanding cascade reaction, the acetic acid to isobutene conversion involves several key reaction steps, and each reaction step needs a certain type of active sites. According to recent studies, $Zn_xZr_yO_z$ catalysts with weak acid−base pairs and Brønsted acid sites exhibit a good activity in the acetic acid to isobutene conversion, where weak Lewis acid−base pairs are related to the ketonization and aldol condensation activity, and Brønsted acid sites are related to the hydrolysis of mesityl oxide to isobutene.[13] However, in the present study, Y/Beta zeolites with exclusive Lewis acid sites, as evidenced by ^{1}H and ^{31}P MAS NMR investigations of adsorbed probe molecules (Figures 6 and 7) also exhibit excellent activity in the acetic acid to isobutene conversion. Considering all the information obtained from the catalytic and spectroscopic investigations, we can summarize the overall reaction mechanism of the acetic acid to isobutene conversion over Y/Beta catalyst shown in Scheme 2.

First, the weak acidic silanol groups of [Si]Beta and the Y_2O_3 species are both active in the acetic acid ketonization, i.e., the first step of the acetic acid to isobutene conversion. However, neither silanol groups nor Y_2O_3 species are active in the conversion of acetic acid to isobutene (Figure 3a), which confirms that Y species in interaction with the [Si]Beta framework (Figure 3c) are responsible for the catalytic activity. Subsequently, the formed acetone can easily desorb from the silanol groups or Y sites, and a small part of these molecules can escape as reaction products (as observed both in the catalytic results in Figures 2 and 4 and the TPSR results in Figure 8a), while others are further involved in the aldol condensation reaction to produce diacetone alcohol and mesityl oxide, mainly on Y sites. Meanwhile, water molecules can desorb as byproducts (as supported by TPSR profiles in Figure 8a), or remain on the surface until the cracking reaction occurs, while carbon dioxide are mostly desorbed as gaseous products (as supported by catalytic results in Figures 2 and 4 and the TPSR results in Figure 8a). Additionally, an equilibrium reaction of acetone and diacetone alcohol occurs (Figure 10b), in line with previous studies of acetone conversion over acid catalysts and alkali metal ion-exchanged Beta zeolites.[10,40]

At last, isobutene is produced via mesityl oxide cracking on weakly acidic Si−OH groups and the confined Y species in the presence of water, which is generated by the acetic acid ketonization or diacetone alcohol dehydration. This mechanism is different from the acetic acid conversion over $Zn_xZr_yO_z$ catalysts,[13] where Brønsted acid sites are responsible for this process. However, with the presence of Brønsted acid sites, the further reactions of isobutene, e.g., isomerization reaction to 1- or 2-butenes, and polymerization reactions to aromatics or larger coke compounds, would also occur, which could greatly decrease the selectivity to isobutene and the lifetime of the catalysts.[4,40] Therefore, the absence of Brønsted acid sites in the Y/Beta catalysts under study can greatly suppress the further reactions of isobutene, and consequently, generate a ~60% isobutene yield, corresponding to 90% of the theoretical maximum. On the other side, the coupling products of acetone, e.g., mesityl oxide and other large molecules, would strongly adsorb on Lewis acidic Y species even at high reaction temperatures (Figure 9, which could lead a gradual coverage of the active Y species, and cause the catalyst deactivation eventually (not shown).

DOI: 10.1021/acscatal.9b02850
ACS Catal. 2019, 9, 9726−9738

The proposed mechanism in Scheme 2 illustrates that for a rational design of an eligible catalyst for the cascade reaction of acetic acid conversion to isobutene, the functional sites should be well designed and balanced. The strong Brønsted acid sites could be replaced by the weak acidic sites to suppress the further reactions of isobutene, and thus enhance the isobutene selectivity. On the other hand, the strength of the Lewis acid sites should be moderate to weaken the adsorption of the oxygen-containing intermediates, and consequently prolong the catalyst lifetime. Here, with the absence of Brønsted acid sites, weakly acidic Si−OH groups and Lewis acidic Y sites in Y/Beta catalyst could exhibit a good synergistic effect in the acetic acid to isobutene conversion, and this finding provides new possibilities for versatile catalysts in future.

4. CONCLUSIONS

In summary, Lewis acidic Y clusters were created by using zeolite [Si]Beta with structural confinement effect as a catalyst support. Y/Beta zeolite with an enhanced density of weak acidic silanols and the confined Lewis acidic Y clusters exhibited a state-of-the-art isobutene yield of 60%, corresponding to 90% of the theoretical maximum. The reaction mechanism of the acetic acid to isobutene conversion over the Y/Beta catalyst was elucidated and the independent roles of silanols and Y species in this process were clarified. Complementary methods, TPSR, TP-UV−vis, and in situ DRIFTS, illustrate that the following steps are mainly involved in the acetic acid to isobutene conversion: First acetic acid ketonization to acetone, then acetone coupling to diacetone alcohol, followed by dehydration to mesityl oxide, and finally mesityl oxide hydrolysis to isobutene.

Different from the previous studies of $Zn_xZr_yO_z$ catalysts, the weak acidic silanol groups of [Si]Beta zeolite are both active in the acetic acid ketonization and mesityl oxide hydrolysis, while Lewis acidic Y species are active in the aldol condensation of acetone and the mesityl oxide hydrolysis. With the combination of these two functional sites in one catalyst, i.e. Y/Beta, a synergistic effect could be well embodied and an enhancement of the isobutene yield could be achieved. In addition, the structural confinement effects of [Si]Beta zeolite also increase the chance of the acetone intermediates to react with each other on the Y species to generate isobutene rather than escape as unwanted byproducts, which also contributes the enhancement of the isobutene yield. These results provide some fundamental guidelines to multifunctional catalysts for the cascade reaction of acetic acid to isobutene.

■ ASSOCIATED CONTENT

Supporting Information

The Supporting Information is available free of charge on the ACS Publications website at DOI: 10.1021/acscatal.9b02850.

Additional catalyst characterization and UV−vis spectra of the adsorbed organic species (PDF)

■ AUTHOR INFORMATION

Corresponding Authors

*E-mail: weilidai@nankai.edu.cn.
*E-mail: lild@nankai.edu.cn.

ORCID

Weili Dai: 0000-0001-5752-0662
Michael Hunger: 0000-0002-1870-2743
Landong Li: 0000-0003-0998-4061

Notes

The authors declare no competing financial interest.

■ ACKNOWLEDGMENTS

This work was supported by the National Natural Science Funds of China (21872072, 21421001), Municipal Natural Science Funds of Tianjin (18JCJQJC47400, 18JCZDJC37400), 111 Project (B18030), and the Fundamental Research Funds for the Central Universities.

■ REFERENCES

(1) Sun, J.; Zhu, K.; Gao, F.; Wang, C.; Liu, J.; Peden, C. H. F.; Wang, Y. Direct Conversion of Bio-ethanol to Isobutene on Nanosized $Zn_xZr_yO_z$ Mixed Oxides with Balanced Acid-Base Sites. *J. Am. Chem. Soc.* **2011**, *133*, 11096−11099.

(2) Sheldon, R. A. Green and Sustainable Manufacture of Chemicals from Biomass: State of the Art. *Green Chem.* **2014**, *16*, 950−963.

(3) Sun, J.; Wang, Y. Recent Advances in Catalytic Conversion of Ethanol to Chemicals. *ACS Catal.* **2014**, *4*, 1078−1090.

(4) Sun, J.; Baylon, R. A. L.; Liu, C.; Mei, D.; Martin, K. J.; Venkitasubramanian, P.; Wang, Y. Key Roles of Lewis Acid-Base Pairs on $Zn_xZr_yO_z$ in Direct Ethanol/Acetone to Isobutene Conversion. *J. Am. Chem. Soc.* **2016**, *138*, 507−517.

(5) Baylon, R. A. L.; Sun, J.; Martin, K. J.; Venkitasubramanian, P.; Wang, Y. Beyond Ketonization: Selective Conversion of Carboxylic Acids to Olefins over Balanced Lewis Acid-Base Pairs. *Chem. Commun.* **2016**, *52*, 4975−4978.

(6) Liu, C.; Karim, A. M.; Lebarbier, V. M.; Mei, D.; Wang, Y. Vapor Phase Ketonization of Acetic Acid on Ceria Based Metal Oxides. *Top. Catal.* **2013**, *56*, 1782−1789.

(7) Snell, R. W.; Shanks, B. H. Insights into the Ceria-Catalyzed Ketonization Reaction for Biofuels Applications. *ACS Catal.* **2013**, *3*, 783−789.

(8) Pacchioni, G. Ketonization of Carboxylic Acids in Biomass Conversion over TiO_2 and ZrO_2 Surfaces: A DFT Perspective. *ACS Catal.* **2014**, *4*, 2874−2888.

(9) Hutchings, G. J.; Johnston, P.; Lee, D. F.; Williams, C. D. Acetone Conversion to Isobutene in High Selectivity Using Zeolite β Catalyst. *Catal. Lett.* **1993**, *21*, 49−53.

(10) Panov, A. G.; Fripiat, J. J. Acetone Condensation Reaction on Acid Catalysts. *J. Catal.* **1998**, *178*, 188−197.

(11) Biaglow, A. I.; Sepa, J.; Gorte, R. J.; White, D. A ^{13}C NMR Study of the Condensation Chemistry of Acetone and Acetaldehyde Adsorbed at the Brønsted Acid Sites in H-ZSM-5. *J. Catal.* **1995**, *151*, 373−384.

(12) Dolejšek, Z.; Nováková, J.; Bosácek, V.; Kubelková, L. Reaction of Ammonia with Surface Species Formed from Acetone on a HZSM-5 Zeolite. *Zeolites* **1991**, *11*, 244−247.

(13) Crisci, A. J.; Dou, H.; Prasomsri, T.; Román-Leshkov, Y. Cascade Reactions for the Continuous and Selective Production of Isobutene from Bioderived Acetic Acid Over Zinc-Zirconia Catalysts. *ACS Catal.* **2014**, *4*, 4196−4200.

(14) Liu, C.; Sun, J.; Smith, C.; Wang, Y. A Study of $Zn_xZr_yO_z$ Mixed Oxides for Direct Conversion of Ethanol to Isobutene. *Appl. Catal., A* **2013**, *467*, 91−97.

(15) Dai, W.; Zhang, S.; Yu, Z.; Yan, T.; Wu, G.; Guan, N.; Li, L. Zeolite Structural Confinement Effects Enhance One-Pot Catalytic Conversion of Ethanol to Butadiene. *ACS Catal.* **2017**, *7*, 3703−3706.

(16) Yan, T.; Dai, W.; Wu, G.; Lang, S.; Hunger, M.; Guan, N.; Li, L. Mechanistic Insights into One-Step Catalytic Conversion of Ethanol to Butadiene over Bifunctional Zn-Y/Beta Zeolite. *ACS Catal.* **2018**, *8*, 2760−2773.

(17) Tang, B.; Dai, W.; Wu, G.; Guan, N.; Li, L.; Hunger, M. Improved Post-Synthesis Strategy to Sn-Beta Zeolites as Lewis Acid Catalysts for the Ring-Opening Hydration of Epoxides. *ACS Catal.* **2014**, *4*, 2801−2810.

DOI: 10.1021/acscatal.9b02850
ACS Catal. 2019, 9, 9726−9738

(18) Tang, B.; Dai, W.; Sun, X.; Guan, N.; Li, L.; Hunger, M. A Procedure for the Preparation of Ti-Beta Zeolites for Catalytic Epoxidation with Hydrogen Peroxide. *Green Chem.* **2014**, *16*, 2281−2291.
(19) Yuan, E.; Dai, W.; Wu, G.; Guan, N.; Hunger, M.; Li, L. Facile Synthesis of Sn-Containing MFI Zeolites as Versatile Solid Acid Catalysts. *Microporous Mesoporous Mater.* **2018**, *270*, 265−273.
(20) Muller, P.; Burt, S. P.; Love, A. M.; McDermott, W. P.; Wolf, P.; Hermans, I. Mechanistic Study on the Lewis Acid Catalyzed Synthesis of 1,3-Butadiene over Ta-BEA Using Modulated Operando DRIFTS-MS. *ACS Catal.* **2016**, *6*, 6823−6832.
(21) Martinez, R.; Huff, M. C.; Barteau, M. A. Ketonization of Acetic Acid on Titania-Functionalized Silica Monoliths. *J. Catal.* **2004**, *222*, 404−409.
(22) Yan, T.; Yang, L.; Dai, W.; Wang, C.; Wu, G.; Guan, N.; Hunger, M.; Li, L. On the Deactivation Mechanism of Zeolite Catalyst in Ethanol to Butadiene Conversion. *J. Catal.* **2018**, *367*, 7−15.
(23) Yang, L.; Yan, T.; Wang, C.; Dai, W.; Wu, G.; Hunger, M.; Fan, W.; Xie, Z.; Guan, N.; Li, L. Role of Acetaldehyde in the Roadmap from Initial Carbon-Carbon Bonds to Hydrocarbons during Methanol Conversion. *ACS Catal.* **2019**, *9*, 6491−6501.
(24) Bennett, J. A.; Parlett, C. M. A.; Isaacs, M. A.; Durndell, L. J.; Olivi, L.; Lee, A. F.; Wilson, K. Acetic Acid Ketonization over Fe_2O_3/SiO_2 for Pyrolysis Bio-Oil Upgrading. *ChemCatChem* **2017**, *9*, 1648−1654.
(25) Zhao, P.; Ye, L.; Sun, Z.; Lo, B. T. W.; Woodcock, H.; Huang, C.; Tang, C.; Kirkland, A. I.; Mei, D.; Edman Tsang, S. C. Entrapped Single Tungstate Site in Zeolite for Cooperative Catalysis of Olefin Metathesis with Brønsted Acid Sites. *J. Am. Chem. Soc.* **2018**, *140*, 6661−6667.
(26) Chen, G.; Dong, M.; Li, J.; Wu, Z.; Wang, G.; Qin, Z.; Wang, J.; Fan, W. Self-Metathesis of 1-Butene to Propene over SBA-15-Supported WO_3. *Catal. Sci. Technol.* **2016**, *6*, 5515−5525.
(27) Xu, Q.; Yang, W.; Chen, Z.; Ye, Y.; Luo, Y.; Street, J.; Zhou, H.; Xu, C. Formation and Regeneration of Shape-Selective ZSM-35 Catalysts for *n*-Butene Skeletal Isomerization to Isobutene. *ACS Omega* **2018**, *3*, 8202−8211.
(28) Pham, T. N.; Sooknoi, T.; Crossley, S. P.; Resasco, D. E. Ketonization of Carboxylic Acids: Mechanisms, Catalysts, and Implications for Biomass Conversion. *ACS Catal.* **2013**, *3*, 2456−2473.
(29) Tosoni, S.; Pacchioni, G. Acetic Acid Ketonization on Tetragonal Zirconia: Role of Surface Reduction. *J. Catal.* **2016**, *344*, 465−473.
(30) Yamada, Y.; Segawa, M.; Sato, F.; Kojima, T.; Sato, S. Catalytic Performance of Rare Earth Oxides in Ketonization of Acetic Acid. *J. Mol. Catal. A: Chem.* **2011**, *346*, 79−86.
(31) Yu, D.; Dai, W.; Wu, G.; Guan, N.; Li, L. Stabilizing Copper Species Using Zeolite for Ethanol Catalytic Dehydrogenation to Acetaldehyde. *Chin. J. Catal.* **2019**, *40*, 1375−1384.
(32) Tang, B.; Dai, W.; Sun, X.; Wu, G.; Guan, N.; Hunger, M.; Li, L. Mesoporous Zr-Beta Zeolite Prepared by Post-Synthetic Strategy as a Robust Lewis Acid Catalyst for the Ring-Opening Aminolysis of Epoxides. *Green Chem.* **2015**, *17*, 1744−1755.
(33) Tang, B.; Dai, W.; Sun, X.; Wu, G.; Li, L.; Guan, N.; Hunger, M. Incorporation of Cerium Atoms into Al-free Beta Zeolite Framework for Catalytic Application. *Chin. J. Catal.* **2015**, *36*, 801−805.
(34) Hasan, M. A.; Zaki, M. I.; Pasupulety, L. Oxide-Catalyzed Conversion of Acetic Acid into Acetone: An FTIR Spectroscopic Investigation. *Appl. Catal., A* **2003**, *243*, 81−92.
(35) Li, H.; Sun, J.; Wang, Y. Surface Acetone Reactions on ZnxZryOz: A DRIFTS-MS Study. *Appl. Catal., A* **2019**, *573*, 22−31.
(36) Zaki, M. I.; Hasan, M. A.; Al-Sagheer, F. A.; Pasupulety, L. Surface Chemistry of Acetone on Metal Oxides: IR Observation of Acetone Adsorption and Consequent Surface Reactions on Silica-Alumina versus Silica and Alumina. *Langmuir* **2000**, *16*, 430−436.
(37) Quesada, J.; Faba, L.; Díaz, E.; Bennici, S.; Auroux, A.; Ordóñez, S. Role of Surface Intermediates in the Deactivation of Mg-Zr Mixed Oxides in Acetone Self-Condensation: A Combined DRIFT and ex situ Characterization Approach. *J. Catal.* **2015**, *329*, 1−9.
(38) Herrmann, S.; Iglesia, E. Elementary Steps in Acetone Condensation Reactions Catalyzed by Aluminosilicates with Diverse Void Structures. *J. Catal.* **2017**, *346*, 134−153.
(39) Herrmann, S.; Iglesia, E. Selective Conversion of Acetone to Isobutene and Acetic Acid on Aluminosilicates: Kinetic Coupling between Acid-Catalyzed and Radical-Mediated Pathways. *J. Catal.* **2018**, *360*, 66−80.
(40) Tago, T.; Konno, H.; Ikeda, S.; Yamazaki, S.; Ninomiya, W.; Nakasaka, Y.; Masuda, T. Selective Production of Isobutylene from Acetone over Alkali Metalion-Exchanged BEA Zeolites. *Catal. Today* **2011**, *164*, 158−162.
(41) Korhonen, S. T.; Calatayud, M.; Krause, A. O. I. Structure and Stability of Formates and Carbonates on Monoclinic Zirconia: A Combined Study by Density Functional Theory and Infrared Spectroscopy. *J. Phys. Chem. C* **2008**, *112*, 16096−16102.
(42) Rotzinger, F. P.; Kesselman-Truttmann, J. M.; Hug, S. J.; Shklover, V.; Grätzel, M. Structure and Vibrational Spectrum of Formate and Acetate Adsorbed from Aqueous Solution onto the TiO_2 Rutile (110) Surface. *J. Phys. Chem. B* **2004**, *108*, 5004−5017.
(43) Tago, T.; Konno, H.; Sakamoto, M.; Nakasaka, Y.; Masuda, T. Selective synthesis for light olefins from acetone over ZSM-5 zeolites with nano- and macro-crystal sizes. *Appl. Catal., A* **2011**, *403*, 183−191.
(44) McAllister, S. H.; Bailey, W. A.; Bouton, C. M. The Catalyzed Cleavage of Diacetone Alcohol and Other Ketols and Unsaturated Ketones. *J. Am. Chem. Soc.* **1940**, *62*, 3210−3215.

DOI: 10.1021/acscatal.9b02850
ACS Catal. 2019, 9, 9726−9738